

10/20/92 850

Conf - 920315 - - 12

SLAC-PUB--5766

DE92 011584

THE COUPLED DIPOLE MODES OF THE NLC ACCELERATOR STRUCTURE*

K.L.F. Bane, R. Gluckstern^o and N. Holtkamp[†]

Stanford Linear Accelerator Center, Stanford University, Stanford, CA 94309 USA

INTRODUCTION

The proposed accelerator cavity of the Next Linear Collider (NLC) [1] is a disk-loaded structure composed of 200 cells, operating at 11.42 GHz. The proposed mode of operation is to accelerate bunches in trains of 10, with a bunch spacing of 42 cm. One problem is that one bunch in a train can excite transverse wakefields in the accelerator cavity which, in turn, can deflect following bunches and result in emittance growth. A method of curing this problem is to detune the transverse modes of the cavity [2].

Beam dynamics simulations for the NLC have shown that by keeping the transverse wakefield at the positions of the nine trailing bunches at or below 1 MV/nC/m² we can avoid emittance growth [3]. Earlier, approximate calculations of the wakefields, which did not include the cell-to-cell coupling of the modes, have shown that by the proper Gaussian detuning the above level of cancellation can be achieved [2,4]. A specific goal of this report is to see if this conclusion still holds when coupling is included in the calculation. Note that in this paper we focus on the modes belonging to the first dipole passband, which are the most important. A special feature of these modes in the detuned NLC cavity is that the cell-to-cell coupling changes sign somewhere in the middle of the structure.

We model the detuned cavity by a chain of coupled resonant circuits, with each loop of the chain representing one cavity cell. The constants in the equation we obtain by fitting to results obtained by TRANSVRS, a computer program that solves Maxwell's equations in a periodic disk-loaded structure [5]. By solving a matrix eigenvalue problem we obtain the frequencies and kick factors of the normal modes of the cavity which, in turn, give us the wakefield. We then repeat the process using a double band of circuits to model the cavity, which duplicates the dispersion curves of the lowest two bands more accurately.

Early examples describing the use of equivalent circuits for finding the normal modes of a multi-cell cavity are given in Refs. [6-8]. As in Ref. [8] our single circuit chain couples through mutual inductors. Recently M. Drevlak [9] applied equivalent circuits that couple through inductors or capacitors to an S-band cavity to find the modes and the wakefields. His circuit models are applicable to structures for which the coupling does not change sign within the cavity. K. Bane and N. Holtkamp [10] using a more complicated circuit, solve a non-linear eigenvalue problem, to find modes of the NLC detuned cavity. A preliminary version of the present work was presented by R. Miller at Protvino in September 1991 [11]. Finally Yamamoto *et al.* [12] apply direct time domain integration of the circuits to find the wakefield of the JLC detuned cavity (a similar cavity), confirming the results presented here.

More details of our results can be found in Ref. [13].

*Work supported by Department of Energy contract DE-AC03-76SF00515.

^oVisitor from the University of Maryland.

[†]Visitor from DESY.

MASTER

Contributed to the 3rd European Particle Accelerator Conference, Berlin, Germany, March 24-28, 1992

DISTRIBUTION OF THIS DOCUMENT IS UNLIMITED 2B

The Uncoupled Calculation of the Wakefield

The dipole wakefield of a cavity is given by a sum over the modes (see, for example, Ref. [14])

$$W(s) = 2 \sum_p K_p \sin \frac{2\pi\nu_p s}{c} \quad s > 0, \quad (1)$$

with K_p the kick factor and ν_p the frequency of the p^{th} dipole mode of the structure. Here we assume that the Q 's of the modes are sufficiently high so that (for our purposes) the damping of the modes can be ignored. Note that for a detuned structure the sum in Eq. (1), for small s , can be replaced by an integral. If the frequency distribution is Gaussian, with rms width σ_{ν} and average $\bar{\nu}$ then

$$W(s) \approx 2\bar{\nu} s \sin \frac{2\pi\bar{\nu} s}{c} e^{-2(\pi\sigma_{\nu}s/c)^2} \quad (2)$$

The method that to date has been used to obtain the wakefield of a detuned version of the NLC accelerator cavity we call the *uncoupled* solution. According to this calculation the wakefield of an N -cell detuned structure is approximated by [4]

$$W(s) = \frac{2}{N} \sum_m^N K_s^{(m)} \sin \frac{2\pi\nu_s^{(m)} s}{c} \quad (3)$$

with N the number of cells. In Eq. (3) $K_s^{(m)}$ and $\nu_s^{(m)}$ represent the kick factor and frequency of the synchronous component of the first dipole mode for a periodic structure with the dimensions of cell m . We expect this approximation to be valid for a short distances s , before the cell-to-cell coupling becomes important.

In this paper we limit ourselves to cell geometries with four parameters: the iris radius a , the cavity radius b , the iris thickness t (= 1.46 mm), and the period L (= 8.75 mm). We detune the structure by varying a and b in such a way as to keep the fundamental frequency at 11.42 GHz. To find any local property of a detuned cavity we first find that property for 7 representative, periodic structures that span our possible range in cell dimensions using the computer program TRANSVRS. These seven, with labels *A-G*, vary in iris radius from 6.50 mm to 2.75 mm in even steps. We then find that local property for any intermediate dimension by interpolation.

For all our simulations we take the distribution in ν_s to be Gaussian, with rms spread $\sigma_{\nu_s}/\bar{\nu}_s = 2.5\%$ and average $\bar{\nu}_s = 15.25$ GHz, and N to be 200. For these parameters the uncoupled calculation gives the wake envelope $\tilde{W}(s)$ shown in Fig. 1. The dashed curve (in all our wakefield plots) displays the Gaussian envelope of Eq. (2) for comparison. We note that the wake satisfies our criterion ≤ 1 MV/nC/m² at the positions of bunches 2-10.

SINGLE CHAIN OF COUPLED CIRCUITS

We consider the circuit chain shown in Fig. 2. For loop m of the circuit we can write

$$\left(\frac{1}{\nu_m^2} - \frac{1}{\nu^2} \right) f_m + \frac{\kappa_{m+\frac{1}{2}}}{2} f_{m+1} + \frac{\kappa_{m-\frac{1}{2}}}{2} f_{m-1} = 0 \quad (4)$$

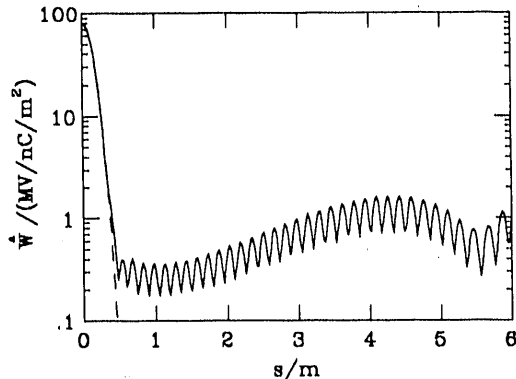


Fig. 1. The wakefield envelope for the uncoupled solution.

with ν the eigenfrequencies of the circuit chain; with ν_m the cell frequency and $\kappa_{m\pm\frac{1}{2}}$ the cell-to-cell coupling for cell m . The eigenfunctions are given by

$$f_m \equiv i_m / \sqrt{C_m} , \quad (5)$$

where, for loop m , i_m is the Fourier transform of the current and C_m is the capacitance. We will allow $\kappa_{m\pm\frac{1}{2}}$ to be a positive or negative quantity depending on whether locally the cell-to-cell coupling is positive or negative. For N circuits Eq. (4) represents a linear, symmetric eigenvalue (ν^{-2}) eigenfunction (f_m) problem of dimension N . Typically the cavity has N full cells ($m = 1, \dots, N$) with the end cells connected to side tubes for which the modes are below cut-off. We therefore take as boundary conditions

$$f_0 = f_1 , \quad f_{N+1} = f_N , \quad \kappa_{\frac{1}{2}} = \kappa_1 , \quad \kappa_{N+\frac{1}{2}} = \kappa_N . \quad (6)$$

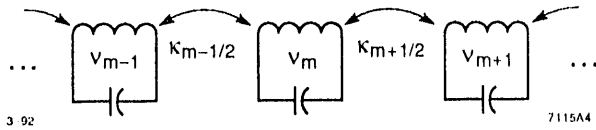


Fig. 2. Our single chain circuit model.

If we substitute constant $\nu_m = \bar{\nu}$ and $\kappa_{m\pm\frac{1}{2}} = \kappa$ into Eq. (4) we then obtain the periodic solutions:

$$f_m = f \cos m\phi \quad \text{and} \quad \frac{1}{\nu^2} = \frac{1}{\bar{\nu}^2} + \kappa \cos \phi . \quad (7)$$

We see that ν^{-2} is linear with $\cos \phi$. We find the dependence on geometry of ν_m and κ_m by fitting to TRANSVRS results. The fit, for periodic cavities with dimensions A-G, is shown in Fig. 3. Since we fit at the ends of the curves the agreement is quite good in the important vicinity of the synchronous point.

The kick factor for mode p is given by

$$K_p = \frac{|\sum_n f_n^{(p)} \sqrt{K_s^{(n)} \nu_s^{(n)} e^{in\varphi_p}}|^2}{N \nu_p \sum_n f_n^{(p)2}} , \quad (8)$$

with $\varphi_p = 2\pi\nu_p L/c$ the phase shift per cell. Doing the numerical calculations we obtain for the detuned NLC cavity the wake envelope shown in Fig. 4. We see that for $0.40 \text{ m} < s < 3.80 \text{ m}$ the cancellation is slightly better than for the uncoupled result. Since the double chain model gives similar results we will wait until the next section to give more details.

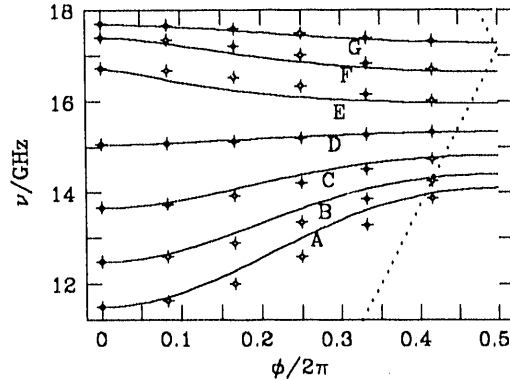


Fig. 3. The single circuit chain solutions with 6 identical cells (the plotting symbols) and the TRANSVRS dispersion curves. The dots give the speed of light line.

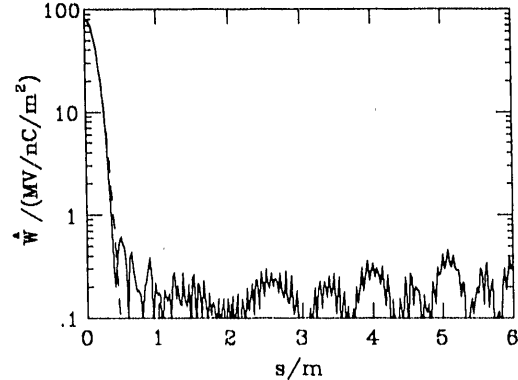


Fig. 4. The wakefield envelope for the single-circuit chain model.

DOUBLE CHAIN OF COUPLED CIRCUITS

In an effort to put the difference equations on a more physical basis we expand the fields in each cell into a combination of a TM_{110} and a TE_{111} mode, and relate the coefficients in adjacent cells to one another by treating the iris coupling using the static approximation of Bethe [15]. The details are presented in Ref. [13]. We then obtain

$$(x_m - \lambda) f_m - \frac{\kappa_{m+\frac{1}{2}}}{2} f_{m+1} - \frac{\kappa_{m-\frac{1}{2}}}{2} f_{m-1} = - \frac{\sqrt{\kappa_{m+\frac{1}{2}} \kappa_{m+\frac{1}{2}}}}{2} \hat{f}_{m+1} + \frac{\sqrt{\kappa_{m-\frac{1}{2}} \kappa_{m-\frac{1}{2}}}}{2} \hat{f}_{m-1} \quad (9)$$

$$(\hat{x}_m - \lambda) \hat{f}_m + \frac{\hat{\kappa}_{m+\frac{1}{2}}}{2} \hat{f}_{m+1} + \frac{\hat{\kappa}_{m-\frac{1}{2}}}{2} \hat{f}_{m-1} = + \frac{\sqrt{\kappa_{m+\frac{1}{2}} \kappa_{m+\frac{1}{2}}}}{2} f_{m+1} - \frac{\sqrt{\kappa_{m-\frac{1}{2}} \kappa_{m-\frac{1}{2}}}}{2} f_{m-1} , \quad (10)$$

with $\lambda \equiv 1/\nu^2$; with f_m and \hat{f}_m representing respectively the TM_{110} and the TE_{111} part of the mode. The equivalent circuit representation of Eqs. (9), (10), includes two bands, with cross-coupling only between adjacent cells. We obtain the parameters x_m , \hat{x}_m , $\kappa_{m\pm\frac{1}{2}}$, $\hat{\kappa}_{m\pm\frac{1}{2}}$, by fitting to TRANSVRS results. Eqs. (9), (10), represent a symmetric eigenvalue problem with $2N$ eigenvalues and $2N$ eigenfunctions. At the ends of the structure we take symmetric boundary conditions for the f 's and anti-symmetric ones

for the \hat{f} 's. For a periodic structure we obtain the dispersion relation

$$\cos \phi = \frac{\kappa \hat{\kappa} - (x - \lambda)(\hat{x} - \lambda)}{(x - \lambda)\hat{\kappa} - (\hat{x} - \lambda)\kappa} \quad (11)$$

When plotted as $\cos \phi$ against λ , Eq. (11) is a hyperbola with one horizontal asymptote. Figure 5 shows the fit of the model to the dispersion curves for geometries A-G.

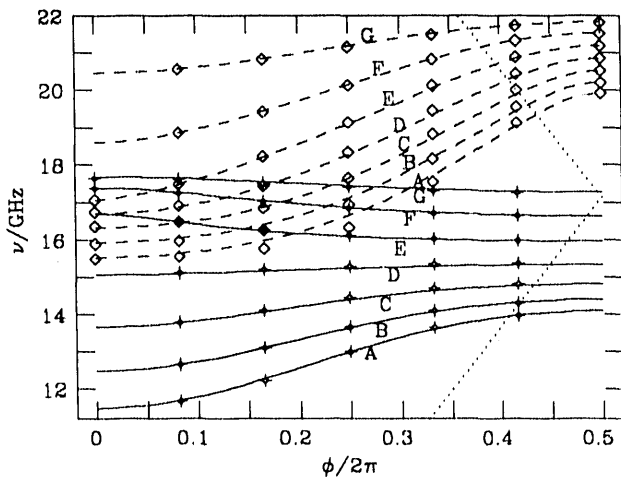


Fig. 5. The double circuit chain solutions with 6 identical cells (the plotting symbols) and the TRANSVRS dispersion curves. The dots give the speed of light line.

We have repeated the calculation for the NLC detuned cavity, using the two band model. In our discussion we will focus on the properties of the first band modes, since they dominate. Most of the modes are localized in the cavity, some in only a few cells (as was also found in Ref. [10]). Two example mode patterns as function of cell number m are shown in Fig. 6. Figure 7 summarizes all the results. We plot the frequency distribution (a), the kick factors (b), the product of these two functions (c), which, when shifted, gives the Fourier transform of the short range wake. The dashes [in (a)-(c)] connect the solution of the uncoupled calculation. Note that the beginnings of a second peak seen in frame (a) are modes belonging to the second dipole passband. In frame (d) we plot the wake. We see again that it is acceptable for our needs. We find this result to be insensitive to the choice of boundary conditions. Finally, in Fig. 8 we show the kick profile V_m seen by bunch number n_b = 2 and n_b = 10 as they traverse the 200 cells. The area under this curve gives the wakefield seen by the bunch.

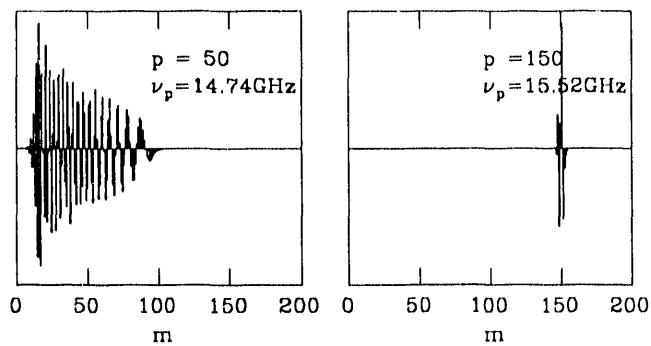


Fig. 6. Mode patterns for modes 50 and 150.

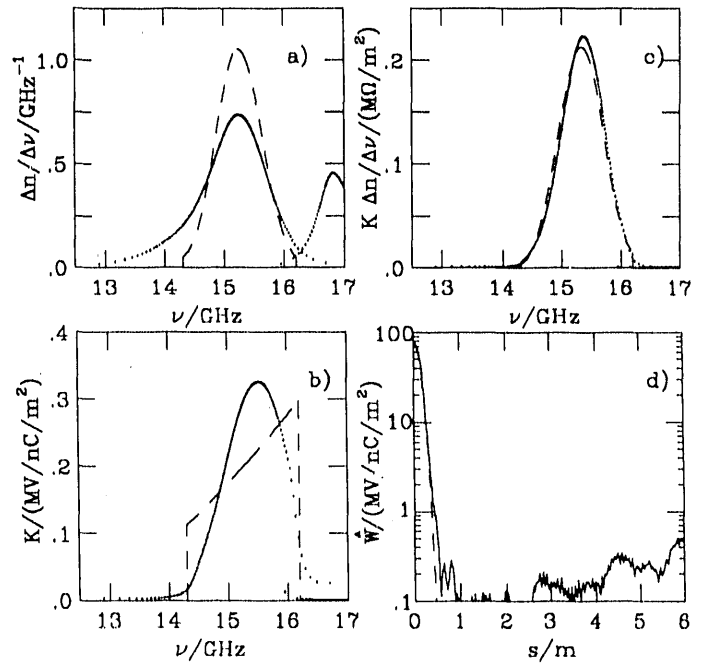


Fig. 7. Double chain results for the NLC cavity.

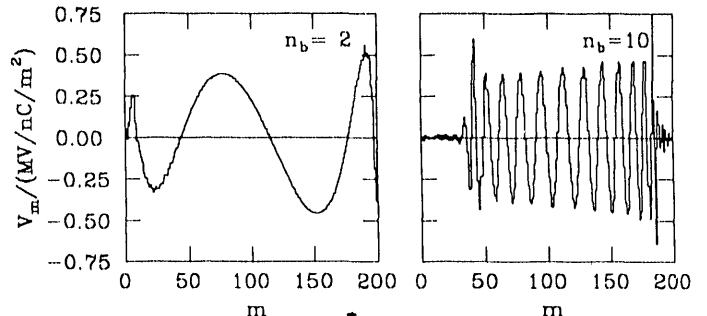


Fig. 8. The kick profile for bunches 2 and 10.

REFERENCES

- [1] R. Ruth, SLAC PUB-5729, March 1992.
- [2] H. Deruyter *et al.*, Proceedings of the 1990 Linear Accelerator Conf., Albuquerque, NM, p. 132, 1990.
- [3] K.A. Thompson, private communication.
- [4] K.A. Thompson and J.W. Wang, Proc. of the 1991 IEEE Part. Accl. Conf., San Francisco, p. 431, 1991.
- [5] K. Bane and B. Zotter, Proceedings of the 11th Int. Conf. on High Energy Accelerators, CERN, p. 581.
- [6] T.I. Smith, HEPL 437, Stanford University, 1966.
- [7] D.E. Nagle *et al.*, *Rev. Sci. Instrum.* **38**, 1583 (1967).
- [8] J. Rees, PEP Note 255, SLAC, 1976.
- [9] M. Drevlak, Thesis, Technische Hochschule Darmstadt, Darmstadt, Germany, December 1991.
- [10] K. Bane and N. Holtkamp, SLAC-AAS-63, Sept. 1991.
- [11] R. Miller, oral presentation at the ECFA Workshop on e^+e^- Linear Colliders, Protvino, Russia, September 1991.
- [12] M. Yamamoto *et al.*, KEK preprint 91-153, Nov. 1991.
- [13] K. Bane and R. Gluckstern, SLAC-PUB 5783, Mar. 1992.
- [14] K. Bane, T. Weiland, P.B. Wilson, in *Physics of High Energy Particle Accelerators*, AIP Conf. Proc. No. 127, 1983.
- [15] H.A. Bethe, *Phys. Rev.* **66**, 163 (1944).

END

DATE
FILMED
6/05/92

